International Journal of Pure and Applied Mathematics
Volume 88 No. 2 2013, 273-295
ISSN: 1311-8080 (printed version); ISSN: 1314-3395 (on-line version)
url: http://www.ijpam.eu
doi: http://dx.doi.org/10.12732/ijpam.v88i2.10

HIGH ORDER METHOD FOR SINGULARLY PERTURBED DIFFERENTIAL-DIFFERENCE EQUATIONS WITH SMALL SHIFTS

A.A. Salama[1], D.G. Al-Amery[2] §

[1,2]Department of Mathematics
Faculty of Science
Assiut University
Assiut, EGYPT

Abstract: This paper deals with a class of singularly perturbed differential-difference equations with small shifts (delay and advance). A high order accurate tridiagonal compact implicit method on non-uniform mesh is developed for approximating the solution of these equations. It is proved that the numerical method has third order of accuracy. The stability analysis and the truncation error are discussed. Several numerical examples are solved to demonstrate the accuracy and the efficiency of the proposed method and how the size of the delay and advance parameters affect the layer behavior of the solution.

AMS Subject Classification: 65L10, 34K26, 76N20
Key Words: singularly perturbed, differential-difference equations, high-order method, boundary layer, Shishkin mesh, small shifts

1. Introduction

In this paper, we consider the following singularly perturbed differential-difference

Received: July 18, 2013

§Correspondence author

equation (SPDDE):

$$Lu_\varepsilon(x) \equiv \varepsilon u''_\varepsilon(x)+a(x)u'_\varepsilon(x)+b(x)u_\varepsilon(x-\delta)+c(x)u_\varepsilon(x)+d(x)u_\varepsilon(x+\eta) = f(x), \quad x \in (0,1),$$

$$\begin{aligned} u_\varepsilon(x) &= \phi(x), \qquad -\delta \le x \le 0, \\ u_\varepsilon(x) &= \psi(x), \qquad 1 \le x \le 1+\eta, \end{aligned} \tag{1.1}$$

where the functions a, b, c, d, f, ϕ and ψ are smooth, $0 < \varepsilon \ll 1$ is the singular perturbation parameter and $0 < \delta, \eta \ll 1$ are the delay and the advance parameters, respectively. A singularly perturbed delay differential equation is an ordinary differential equation in which the highest derivative is multiplied by a small parameter and involving at least one delay term, for details, see [1, 16]. The solution $u_\varepsilon(x)$ of the boundary value problem (1.1) exhibits a single boundary layer at the left (or right) end of the interval $I = (0, 1)$ depending on $a(x) - \delta b(x) + \eta d(x) > 0$ (or < 0).

These equations are widespread in many branches of sciences and engineering and have been used for many years in control theory [4], description of the so-called human pupil-light reflex [13] and evolutionary biology [21]. The arguments for small delay problems are found throughout the literature on epidemics and population where these small shifts play an important role in the modeling of various real life phenomena, see [10]. Many researchers have investigated the effect of small shift on the layer behavior of the solution and observed that it is very small and affects the solution significantly. In this direction, Lange and Miura [11, 12] provided asymptotic approach to SPDDE (1.1) and showed that the effect of the small delay and shift terms on the solution cannot be neglected. The numerical study of singularly perturbed delay differential equations is initiated in [7]. Some of the other relevant references are [6, 9, 15].

It is well known that standard discretization methods for solving singular perturbation problems are not useful and fail to give accurate results when the perturbation parameter ε tends to zero. This motivates the need for other methods that have ε-uniform convergence. In general there are two approaches for construction ε-uniform methods. The first one is the fitted operator method which contains specially designed finite difference operator which reflects the singularly perturbed nature of the solution. An extensive details of ε-uniform fitted operator methods can be found in [3, 14], and references therein. The

second one is the fitted mesh method which contains finite difference operators on specially designed meshes such as nonuniform layer-adapted meshes, Shishkin mesh [14, 18] and grid equidistribution [15, 17].

In this paper we propose numerical method to solve singularly perturbed differential equation with small shifts. To overcome the defect and weakness of the standard methods, we use a piecewise uniform mesh. In this method, we approximate the terms containing small shifts (delay and advance) by Taylor series, then we apply operator compact implicit (OCI) method on non-uniform mesh. Both cases, when boundary layer occurs in left and right side of interval will be studies. We show that the method is useful for obtaining numerical solution of considered problem in both cases. The advantages of this method are that it is simple to implement and it achieves high accuracy comparing with other methods.

In Section 2, we present some properties of the continuous solution of the considered problem. Section 3 is devoted to the numerical method, we present in details the construction of the numerical method. The stability analysis and the truncation error are discussed in Section 4. In Section 5, some numerical examples are presented to show the applicability and the effectiveness of the present method. Finally, conclusion is indicated in Section 6.

2. Continuous Problem

In this section, we consider a boundary-value problem for SPDDE with mixed type of small shifts of the form (1.1). It is noted that if $\delta = \eta = 0$, then (1.1) reduces to the singularly perturbed differential equation (SPDE), which is studied by numerous researchers, see for example [14, 17, 18].

For sufficiently small δ and η, we follow the same technique in [11, 12]. To tackle the shift terms, we expand the shift terms through Taylor series expansions assuming smoothness condition on the solution of (1.1). So that the problem (1.1) reduces to a singular perturbation problem.
Now, using Taylor approximation to expand the delay and advance terms, we obtain

$$\begin{aligned} u_\varepsilon(x-\delta) &= u_\varepsilon(x) - \delta u'_\varepsilon(x) + \tfrac{\delta^2}{2} u''_\varepsilon(x) - \cdots \\ u_\varepsilon(x+\eta) &\approx u_\varepsilon(x) + \eta u'_\varepsilon(x) + \tfrac{\eta^2}{2} u''_\varepsilon(x) + \cdots \end{aligned} \tag{2.1}$$

Using (2.1) in (1.1), we get

$$\begin{aligned} &\tilde{L}u(x) \equiv \varepsilon u''(x) + \tilde{a}(x)u'(x) + \tilde{b}(x)u(x) = \tilde{f}(x), \qquad x \in (0,1) \\ &u(0) = \phi(0), \qquad u(1) = \psi(1), \end{aligned} \tag{2.2}$$

where

$$\tilde{a}(x) = \big(a(x) - \delta b(x) + \eta d(x)\big)/\tilde{c}(x), \qquad \tilde{b}(x) = \big(b(x) + c(x) + d(x)\big)/\tilde{c}(x),$$

$$\tilde{f}(x) = f(x)/\tilde{c}(x), \qquad \tilde{c}(x) = 1 + \big(\delta^2 b(x) + \eta^2 d(x)\big)/2\varepsilon.$$

Note that, since (2.2) is an approximation of (1.1), we have used only $u(x)$ instead of $u_\varepsilon(x)$. Here, we assume that $\tilde{a}(x) \geq K > 0$ and $\tilde{b}(x) \leq -M < 0$ throughout the interval $[0,1]$, where K and M are positive constants. Under these assumptions, the solution of problem (2.2) exhibits a single boundary layer at the left side of the interval.

Lemma 1 (Continuous minimum principle)**.** *Let $u(x)$ be a smooth function satisfying $u(0) \geq 0$ and $u(1) \geq 0$. Then $\tilde{L}u(x) \leq 0$, $\forall x \in I = (0,1)$ implies that $u(x) \geq 0$, $\forall x \in \bar{I} = [0,1]$.*

Proof. Let $x^\star \in \bar{I}$ be such that $u(x^\star) = \min\{u(x), x \in \bar{I}\}$ and $u(x^\star) < 0$. Clearly $x^\star \neq 0, x^\star \neq 1$ and therefore $u'(x^\star) = 0$ and $u''(x^\star) \geq 0$.
Hence

$$\tilde{L}u(x^\star) = \varepsilon u''(x^\star) + \tilde{a}(x^\star)u'(x^\star) + \tilde{b}(x^\star)u(x^\star) \geq 0$$

which contradicts the hypothesis that $\tilde{L}u(x) \leq 0$. Therefore $u(x^\star) \geq 0$. But since $x^\star$ was arbitrary point in $\bar{I}$, so that $u(x) \geq 0, \forall x \in \bar{I}$. □

Lemma 2. *Let $u(x)$ be the solution of the problem (2.2), then*

$$\|u\| \leq M^{-1}\|\tilde{f}\| + \max\{|\phi(0)|, |\psi(1)|\}.$$

Proof. We consider two barrier functions $\chi^{\pm}(x)$ defined by

$$\chi^{\pm}(x) = M^{-1}\|\tilde{f}\| + \max\{|\phi(0)|, |\psi(1)|\} \pm u(x).$$

Then, we have

$$\begin{aligned} \chi^{\pm}(0) = M^{-1}\|\tilde{f}\| + \max\{|\phi(0)|, |\psi(1)|\} \pm u(0) &= M^{-1}\|\tilde{f}\| \\ &+ \max\{|\phi(0)|, |\psi(1)|\} \pm \phi(0) \geq 0, \end{aligned}$$

$$\chi^{\pm}(1) = M^{-1}\|\tilde{f}\| + \max\{|\phi(0)|, |\psi(1)|\} \pm u(1) = M^{-1}|\tilde{f}\| + \max\{|\phi(0)|, |\psi(1)|\} \pm \psi(1) \geq 0,$$

and

$$\begin{aligned}
\tilde{L}\chi^{\pm}(x) &= \varepsilon(\chi^{\pm}(x))'' + \tilde{a}(x)(\chi^{\pm}(x))' + \tilde{b}(x)\chi^{\pm}(x) \\
&= \tilde{b}(x)\big(M^{-1}\|\tilde{f}\| + \max\{|\phi(0)|, |\psi(1)|\}\big) \pm \tilde{L}u(x) \\
&= \tilde{b}(x)\big(M^{-1}\|\tilde{f}\| + \max\{|\phi(0)|, |\psi(1)|\}\big) \pm \tilde{f}(x) \\
&\leq (-\|\tilde{f}\| \pm \tilde{f}(x)) + \tilde{b}(x)\max\{|\phi(0)|, |\psi(1)|\} \\
&\leq 0, \qquad \text{scince}, \|\tilde{f}\| \geq \tilde{f}(x).
\end{aligned}$$

Using Lemma 1, we obtain $\chi^{\pm}(x) \geq 0$ for all $x \in [0, 1]$, which proves the required estimate. □

Lemma 1 implies that the solution of problem (2.2) is unique, and the existence of the solution is implied by its uniqueness and the linearity of the considered problem. Further, the boundedness of the solution is given by Lemma 2.

3. Discretization and Mesh

In this section, we apply the operator compact implicit OCI method [2, 19] for solving (2.2) on a nonuniform grid $\Omega^N = \{x_j\}_{j=1}^N$ and denote $h_j = x_j - x_{j-1}$, where N is a positive integer. Here, we discuss the case when the solution exhibits a single boundary layer at the left side of the interval, i.e. when $\tilde{a}(x) \geq K > 0$. The other case, when a boundary layer occurs in the right side of the interval ($\tilde{a}(x) \leq -K < 0$), one can follow the same procedure as we use for the case of left boundary layer.

To describe the method, we first rewrite SPDE (2.2) in the form

$$\tilde{L}u(x) \equiv \varepsilon u''(x) + \tilde{a}(x)u'(x) = \tilde{F}(x) \tag{3.1}$$

$$u(0) = \phi(0), \qquad u(1) = \psi(1),$$

where $\tilde{F}(x) = \tilde{f}(x) - \tilde{b}(x)u(x)$.
Hence, we define the tridiagonal finite difference method for $\tilde{L}u(x)$ given in above equation by the following

$$\tilde{L}_N U_j \equiv \frac{\varepsilon}{h_j h_{j+1}(h_j + h_{j+1})} R(U_j) = Q(\tilde{F}_j), \qquad j = 1, 2, \cdots, (N-1) \tag{3.2}$$

$$U_0 = \phi(0) \qquad \text{and} \qquad U_N = \psi(1).$$

where

$$\begin{aligned} R(U_j) &= r_j^- U_{j-1} + r_j^c U_j + r_j^+ U_{j+1}, \\ Q(\tilde{F}_j) &= q_j^- \tilde{F}_{j-1} + q_j^c \tilde{F}_j + q_j^+ \tilde{F}_{j+1}, \end{aligned} \tag{3.3}$$

It is worthwhile to mention that U_j and $\tilde{L}_N U_j$ are approximations of $u(x_j)$ and $\tilde{L}u(x_j)$, respectively. The coefficients $r_j^{-,c,+}$ and $q_j^{-,c,+}$ are functions of $h_j, h_{j+1}, \varepsilon$ and $\tilde{a}(x_j)$ as we show later.

3.1. Piecewise-Uniform Shishkin Mesh

It is known that on an uniform mesh no method can achieves convergence at all mesh points uniformly in ε, unless its coefficients have an exponential property which reflects the singularly perturbed nature of the solution. This requires us to use a carefully selected mesh in order to obtain ε-uniform convergence. The simplest non-uniform mesh, namely a piecewise-uniform Shishkin mesh which is dense in the boundary layer region and coarse in the outer region, as $\varepsilon \to 0$. This mesh is attractive because of its efficiency and simplicity for dealing with a wide variety of singularly perturbed problems [14].

Let us consider the the problem (2.2) when $\tilde{a}(x) \geq K > 0$ and $\tilde{b}(x) \leq -M < 0$ throughout the interval $[0, 1]$, where K and M are positive constants. It is clear that due to this assumption the boundary layer occurs near $x = 0$. We divide the domain into two subdomains using $\sigma = \min\{\frac{1}{2}, \frac{8\varepsilon}{K} \ln N\}$. The piecewise-uniform mesh is constructed by dividing the interval $\bar{I} = [0, 1]$ into two subintervals $[0, \sigma]$ and $[\sigma, 1]$, and each of these subintervals is divided into $N/2$ mesh elements of equal length. Therefore, the computational grids are given by

$$x_j = \begin{cases} \frac{2j\sigma}{N}, & 0 \leq j \leq N/2, \\ x_{j-1} + \frac{2(1-\sigma)}{N}, & N/2 < j \leq N, \end{cases}$$

Similarly, the other case when the boundary layer occurs on the right side of the interval, we partition the interval into two subintervals $[0, 1-\sigma]$ and $[1-\sigma, 1]$. The corresponding Shishkin mesh takes the form

$$x_j = \begin{cases} \frac{2j(1-\sigma)}{N}, & 0 \leq j \leq N/2, \\ x_{j-1} + \frac{2\sigma}{N}, & N/2 < j \leq N, \end{cases}$$

3.2. Derivation of the Method

The development of the present method is based on computing the local truncation error as following

$$\tau_j = \tilde{L}_N u(x_j) - Q\big(\tilde{L}u(x_j)\big), \tag{3.4}$$

For the sake of simplicity, we use $\tilde{a}_j = \tilde{a}(x_j), \tilde{a}_{j-1} = \tilde{a}(x_{j-1})$ and $\tilde{a}_{j+1} = \tilde{a}(x_{j+1})$. Since $u(x)$ is sufficiently smooth, and using Taylor expansion, τ_j can be written in the form

$$\tau_j = T_j^0 u(x_j) + T_j^1 u'(x_j) + \cdots + T_j^6 u^{(6)}(x_j) + O(h^5), \quad h = \max\{h_j, h_{j+1}\} \tag{3.5}$$

where

$$\begin{aligned}
T_j^0 &= \frac{\varepsilon}{h_j h_{j+1}(h_j + h_{j+1})}\big(r_j^+ + r_j^c + r_j^-\big)\\
T_j^1 &= \frac{\varepsilon}{h_j h_{j+1}(h_j + h_{j+1})}\Big[h_{j+1} r_j^+ - h_j r_j^-\\
&\quad - \frac{h_j h_{j+1}(h_j + h_{j+1})}{\varepsilon}\big(q_j^+ \tilde{a}_{j+1} + q_j^c \tilde{a}_j + q_j^- \tilde{a}_{j-1}\big)\Big]\\
T_j^2 &= \frac{\varepsilon}{h_j h_{j+1}(h_j + h_{j+1})}\Big[\frac{h_{j+1}^2}{2} r_j^+ + \frac{h_j^2}{2} r_j^- - h_j h_{j+1}(h_j + h_{j+1})\big(q_j^+ + q_j^c + q_j^-\big)\\
&\quad - \frac{h_j h_{j+1}(h_j + h_{j+1})}{\varepsilon}\big(h_{j+1} q_j^+ \tilde{a}_{j+1} - h_j q_j^- \tilde{a}_{j-1}\big)\Big],
\end{aligned}$$

and

$$\begin{aligned}
T_j^k = \frac{\varepsilon}{h_j h_{j+1}(h_j + h_{j+1})}\Bigg\{ &\frac{h_{j+1}^k}{k!} r_j^+ + (-1)^k \frac{h_j^k}{k!} r_j^- - \frac{h_j h_{j+1}(h_j + h_{j+1})}{\varepsilon}\\
&\Big[q_j^+\Big(\frac{h_{j+1}^{k-2}}{(k-2)!}\varepsilon + \frac{h_{j+1}^{k-1}}{(k-1)!}\tilde{a}_{j+1}\Big) + q_j^-\Big((-1)^{k-2}\frac{h_j^{k-2}}{(k-2)!}\varepsilon (-1)^{k-1}\frac{h_j^{k-1}}{(k-1)!}\tilde{a}_{j-1}\Big)\Big]\Bigg\},\\
&k = 3, 4, 5, 6.
\end{aligned} \tag{3.6}$$

The truncation error is said to be of order p if $\tau_j = O(h^p)$ as $h \to 0$ (ε is fixed) for $j = 1, 2, \cdots, (N-1)$. Here, we construct our method by the conditions

$$T_j^k = 0, \qquad k = 0, 1, 2 \tag{3.7}$$

$$T_j^k = O(h^4), \qquad k = 3, 4 \tag{3.8}$$

From conditions (3.7), we obtain

$$\begin{aligned} r_{\mathrm{j}}^{+} &= 2h_{\mathrm{j}}\Big\{q_{\mathrm{j}}^{+}+q_{\mathrm{j}}^{\mathrm{c}}+q_{\mathrm{j}}^{-}+\frac{z}{2}\Big[(1+2\alpha)q_{\mathrm{j}}^{+}\tilde{a}_{\mathrm{j}+1}+q_{\mathrm{j}}^{\mathrm{c}}\tilde{a}_{\mathrm{j}}-q_{\mathrm{j}}^{-}\tilde{a}_{\mathrm{j}-1}\Big]\Big\},\\ r_{\mathrm{j}}^{-} &= 2h_{\mathrm{j}+1}\Big\{q_{\mathrm{j}}^{+}+q_{\mathrm{j}}^{\mathrm{c}}+q_{\mathrm{j}}^{-}+\frac{z}{2}\Big[\alpha q_{\mathrm{j}}^{+}\tilde{a}_{\mathrm{j}+1}-\alpha q_{\mathrm{j}}^{\mathrm{c}}\tilde{a}_{\mathrm{j}}-(2+\alpha)q_{\mathrm{j}}^{-}\tilde{a}_{\mathrm{j}-1}\Big]\Big\},\\ r_{\mathrm{j}}^{\mathrm{c}} &= -r_{\mathrm{j}}^{+}-r_{\mathrm{j}}^{-}, \end{aligned} \tag{3.9}$$

where $z=\frac{h_j}{\varepsilon}$ and $\alpha=\frac{h_{j+1}}{h_j}$. Using equations (3.6) and (3.9) we get

$$\begin{aligned} T_{\mathrm{j}}^{3} =& \frac{\varepsilon h_{\mathrm{j}}}{3!}\Big\{-2(1+2\alpha)q_{\mathrm{j}}^{+}-2(1-\alpha)q_{\mathrm{j}}^{\mathrm{c}}+2(2+\alpha)q_{\mathrm{j}}^{-}\\ &-z\Big[(\alpha+\alpha^{2})q_{\mathrm{j}}^{+}\tilde{a}_{\mathrm{j}+1}-\alpha q_{\mathrm{j}}^{\mathrm{c}}\tilde{a}_{\mathrm{j}}+(1+\alpha)q_{\mathrm{j}}^{-}\tilde{a}_{\mathrm{j}-1}\Big]\Big\}, \end{aligned} \tag{3.10}$$

and

$$\begin{aligned} T_{\mathrm{j}}^{4} =& \frac{\varepsilon h_{\mathrm{j}}^{2}}{4!}\Big\{2\Big[\big(1-\alpha-5\alpha^{2}\big)q_{\mathrm{j}}^{+}+\big(1-\alpha+\alpha^{2}\big)q_{\mathrm{j}}^{\mathrm{c}}-\big(5+\alpha-\alpha^{2}\big)q_{\mathrm{j}}^{-}\Big]\\ &+z\Big[\big(\alpha-\alpha^{2}-2\alpha^{3}\big)q_{\mathrm{j}}^{+}\tilde{a}_{\mathrm{j}+1}+\big(\alpha^{2}-\alpha\big)q_{\mathrm{j}}^{\mathrm{c}}\tilde{a}_{\mathrm{j}}+\big(\alpha-\alpha^{2}+2\big)q_{\mathrm{j}}^{-}\tilde{a}_{\mathrm{j}-1}\Big]\Big\} \end{aligned} \tag{3.11}$$

Now, we define $q_j^{+,c,-}$ as polynomials in z at each mesh point x_j, and for simplifying the notations, the index j in $q_j^{+,c,-}$ will be dropped.

$$q^{+,c,-}=\sum_{i=0}^{3}q_i^{+,c,-}z^i, \tag{3.12}$$

where the coefficients $q_i^{+,c,-}$, $i=0,1,2,3$ are independent of ε. It is well known that (3.12) is well defined in the sense that $q_i^{+,c,-}$ are not all zero as functions of h_j, h_{j+1}. Expression (3.12) implies that $r^{+,c,-}$ are also polynomials in z. Substituting (3.12) into equations (3.10, 3.11) and using (3.8), we obtain the following asymptotic relations as ($h\to 0$, ε is fixed)

$$\begin{aligned} T_j^3 &= \frac{\varepsilon h_j}{3!}\Big[t_0^3+t_1^3z+t_2^3z^2+O(z^3)\Big]=O(h^4)\\ T_j^4 &= \frac{\varepsilon h_j^2}{4!}\Big[t_0^4+t_1^4z+O(z^2)\Big]=O(h^4) \end{aligned}$$

where

$$
\begin{aligned}
t_0^3 &= -2\Big[(1+2\alpha)q_0^+ + (1-\alpha)q_0^c - (2+\alpha)q_0^-\Big] = O(h^3)\\
t_1^3 &= -2\Big[(1+2\alpha)q_1^+ + (1-\alpha)q_1^c - (2+\alpha)q_1^-\Big]\\
&\quad - (\alpha+\alpha^2)q_0^+\tilde{a}_{j+1} + \alpha q_0^c\tilde{a}_j - (1+\alpha)q_0^-\tilde{a}_{j-1} = O(h^2)\\
t_2^3 &= -2\Big[(1+2\alpha)q_2^+ + (1-\alpha)q_2^c - (2+\alpha)q_2^-\Big]\\
&\quad - (\alpha+\alpha^2)q_1^+\tilde{a}_{j+1} + \alpha q_1^c\tilde{a}_j - (1+\alpha)q_1^-\tilde{a}_{j-1} = O(h)\\
t_0^4 &= 2\Big[(1-\alpha-5\alpha^2)q_0^+ + (1-\alpha+\alpha^2)q_0^c - (5+\alpha-\alpha^2)q_0^-\Big] = O(h^2)\\
t_1^4 &= 2\Big[(1-\alpha-5\alpha^2)q_1^+ + (1-\alpha+\alpha^2)q_1^c - (5+\alpha-\alpha^2)q_1^-\Big]\\
&\quad + (\alpha-\alpha^2-2\alpha^3)q_0^+\tilde{a}_{j+1} + (\alpha^2-\alpha)q_0^c\tilde{a}_j + (\alpha-\alpha^2+2)q_0^-\tilde{a}_{j-1} = O(h)
\end{aligned}
\tag{3.13}
$$

Now, we follow the procedure in [2, 19] to determine the coefficients $q_i^{+,c,-}$, $i = 0, 1, 2, 3$.
From equations (3.13), these coefficients are given in the form

$$
\begin{aligned}
&q_0^+ = \frac{\alpha^2+\alpha-1}{\alpha}, \qquad q_0^{\mathrm{c}} = \frac{(1+\alpha)(1+3\alpha+\alpha^2)}{\alpha}, \qquad q_0^- = 1+\alpha-\alpha^2,\\
&q_1^+ = \frac{5+10\alpha+3\alpha^2-2\alpha^3-\alpha^4}{6(1+3\alpha+\alpha^2)}\tilde{a}_{\mathrm{j}}, \quad q_1^{\mathrm{c}} = 0, \quad q_1^- = \frac{1+2\alpha-3\alpha^2-10\alpha^3-5\alpha^4}{6(1+3\alpha+\alpha^2)}\tilde{a}_{\mathrm{j}},\\
&q_2^+ = \frac{1}{16(2\alpha+1)}\Big[(\alpha+2)+2(\alpha-1)+\gamma\Big]\tilde{a}_{\mathrm{j}}^2, \qquad q_2^- = \frac{1}{16}\tilde{a}_{\mathrm{j}}^2, \qquad q_2^{\mathrm{c}} = \frac{1}{8}\tilde{a}_{\mathrm{j}}^2,\\
&q_3^+ = \frac{1}{16}\tilde{a}_{\mathrm{j}}^3, \qquad q_3^{\mathrm{c}} = \frac{1}{16}\tilde{a}_{\mathrm{j}}^2\tilde{a}_{\mathrm{j}+1}, \qquad q_3^- = 0,
\end{aligned}
\tag{3.14}
$$

where

$$
\gamma = \frac{4(\alpha^2-1)(1+8\alpha+15\alpha^2+8\alpha^3+\alpha^4)}{3(1+3\alpha+\alpha^2)}. \tag{3.15}
$$

Then the coefficients, $q^{+,c,-}$ and $r^{+,c,-}$ of the operators Q and R in (3.3) can be computed by (3.12) and (3.9), respectively.

4. Error and Stability Analysis

The local truncation error of the difference method (3.2) at the nodes x_j is given by

$$\tau_j = \tilde{L}_N u(x_j) - Q\big(\tilde{L}u(x_j)\big) = T_j^0 u(x_j) + T_j^1 u'(x_j) + \cdots + T_j^6 u^{(6)}(x_j) + O(h^5),$$

Using equations (3.9), (3.10) and (3.12) and substituting in (3.6), we get

$$T_j^k = 0, \qquad k = 0, 1, 2$$

$$T_j^k = O(h^4), \qquad k = 3, 4, 6$$

and

$$T_j^5 = \frac{\varepsilon}{30h_j}(h_j^2 - h_{j+1}^2)(2h_j + h_{j+1})(h_j + 2h_{j+1}) + O(h^4),$$

Note that, in the case of $h_{j+1} = h_j = h$ the term T_j^5 is of order four ($T_j^5 = O(h^4)$) and the local truncation error is of order four.
Now, we consider the method (3.2) on uniform grid and we assume that $\tilde{a}_j$ is a constant and $\tilde{b}_j = 0$. So that, when $h_{j+1} = h_j$ ($\alpha = 1$), then we obtain the following

$$\tilde{L}_N U_j \equiv \frac{\varepsilon}{h^2} R(U_j) = Q(\tilde{f}_j), \qquad j = 1, 2, \cdots, (N-1) \tag{4.1}$$

$$U_0 = \phi(0) \qquad \text{and} \qquad U_N = \psi(1).$$

where

$$\begin{aligned} R(U_j) &= r_j^- U_{j-1} + r_j^c U_j + r_j^+ U_{j+1}, \\ Q(\tilde{f}_j) &= q_j^- \tilde{f}_{j-1} + q_j^c \tilde{f}_j + q_j^+ \tilde{f}_{j+1}, \end{aligned} \tag{4.2}$$

and

$$\begin{aligned} &q^+ = 1 + \frac{1}{2}\xi + \frac{1}{16}\xi^2 + \frac{1}{16}\xi^3, \quad q^c = 10 + \frac{1}{8}\xi^2 + \frac{1}{16}\xi^3, \quad q^- = 1 - \frac{1}{2}\xi + \frac{1}{16}\xi^2, \\ &r^+ = 12 + 6\xi + \frac{5}{4}\xi^2 + \frac{1}{4}\xi^3 + \frac{1}{8}\xi^4, \quad r^- = 12 - 6\xi + \frac{5}{4}\xi^2, r^c = -(r^+ + r^-), \end{aligned} \tag{4.3}$$

where

$$\xi = \frac{ha_i}{\varepsilon}.$$

Remark 1 In the case of $\tilde{b}_j \neq 0$, our method takes the form

$$\frac{\varepsilon}{h^2} R(U_j) - Q(\tilde{b}_j U_j) = Q(\tilde{f}_j), \qquad j = 1, 2, \cdots, N-1$$

where the operators R, Q and their coefficients are as in (4.2) and (4.3), respectively. Also, this method has the desired properties and achieves fourth-order of convergence.

Lemma 3. *Assume that h is sufficiently small, then the compact difference method defined by* (4.1), (4.2) *and* (4.3) *satisfies the following for $j = 1, 2, \cdots, (N-1)$ and $0 < \frac{h}{\varepsilon} < \infty$*

$$\begin{aligned} & q_i^- \geq 0, \qquad q_i^c \geq 0, \qquad q_i^+ \geq 0, \\ & \textit{and} \\ & r_i^- \geq 0, \qquad r_i^+ \geq 0, \qquad -r_i^c \geq 0. \end{aligned} \tag{4.4}$$

Proof. From (4.3), it is clear that, $q_i^+ > 0, q_i^c > 0$ and $r_i^+ > 0$ for all $\xi \in (0, \infty)$. Now, we show that $q_i^- > 0, r_i^- > 0$ and $-r_i^c \geq 0$. Note that both q_i^- and r_i^- are of the form of quadratic polynomial $a_0 + a_1 x + a_2 x^2$ with $a_0 > 0$, this quadratic is nonnegative on $(0, \infty)$ if and only if: (i) the discriminant is non-positive when $a_1 < 0$ and (ii) $a_2 \geq 0$ when $a_1 \geq 0$. Using this, we find that $q_i^- \geq 0, r_i^- \geq 0$ and $-r_i^c \geq 0$ for all $\xi \in (0, \infty)$. □

Remark 2 It is important to note that, from Lemma 3, the proposed method has no cell Reynolds number limitation. Also note that (4.4) implies that the triadiagonal matrix $\tilde{R}$ associated with the operator R is diagonally dominant with negative main diagonal elements and positive super-diagonal and sub-diagonal elements, and hence $\tilde{R}$ can be inverted, see [5]. This ensures the existence and uniqueness of the solution for the difference method. Moreover, one can observe that r^-/r^+ is the $(4, 2)$ Padé approximation to $e^{-\xi}$. The operator $\tilde{L}_N$ defined in (4.1) satisfies the following

Lemma 4 (Discrete minimum principle)**.** *Suppose $U_0 \geq 0$ and $U_N \geq 0$, and $\tilde{L}_N U_j \leq 0$ for all $j = 1, 2, \cdots, (N-1)$. Then $U_j \geq 0,\ 1 \leq j \leq N-1$.*

Proof. Suppose there exists k, $0 < k < N$ such that $U_k = \min_{0 \leq j \leq N} U_j$ and assume that $U_k < 0$. Then we have

$$\begin{aligned} \tilde{L}_N U_k &= r_k^- U_{k-1} + r_k^c U_k + r_k^+ U_{k+1} = r_k^- U_{k-1} - (r_k^- + r_k^+) U_k + r_k^+ U_{k+1} \\ &= r_k^- (U_{k-1} - U_k) + r_k^+ (U_{k+1} - U_k), \end{aligned}$$

since $(U_{k-1} - U_k) > 0, (U_{k+1} - U_k) > 0, r_j^- > 0$ and $r_j^+ > 0$, then $\tilde{L}_N U_k > 0$ which is a contradiction, and therefore $U_k \geq 0$. Since k is arbitrary, then $U_j \geq 0$ for all $j = 1, 2, \cdots, (N-1)$. □

To show the stability of our method, we first consider the following definition:

Definition A sequence of operators $\tilde{L}_N$ is said to be stable, if the sequence $\tilde{L}_N^{-1}$ is uniformly bounded for sufficiently large N, i.e., if there is an N_0 and a constant C such that

$$\sup_{N>N_0} \|\tilde{L}_N^{-1}\|_2 \leq C < \infty$$

Note that, the operator $\tilde{L}_N$ is an $(N-1)\times(N-1)$ tridiagonal matrix given in (4.1).

Lemma 5. *Let E be the $(N-1)\times(N-1)$ matrix of the form*

$$E = \begin{pmatrix} 0 & 0 & 0 & \cdots & 0 \\ 1 & 0 & 0 & \cdots & 0 \\ 0 & 1 & 0 & \cdots & 0 \\ \vdots & \ddots & \ddots & \ddots & \vdots \\ 0 & \cdots & 0 & 1 & 0 \end{pmatrix}$$

and let $A = -\tilde{\alpha}E + I - \tilde{\beta}E^T$ with I is the identity matrix. Let $\tilde{\alpha}+\tilde{\beta} = 1,\ \alpha, \beta \geq 0$. Then

$$\|A^{-1}\|_2 \leq O\big((N-1)^2\big).$$

Proof. see [20]. □

Theorem 6. *Consider the singularly perturbed boundary value problem* 3.1 *where $\tilde{a}$ is a positive constant and $\tilde{b} = 0$. Let $\tilde{L}_N$ be the $(N-1)\times(N-1)$ difference matrix as defined in* $(4.1 - 4.3)$. *Let $\varepsilon = O(h^p)$, where p is a positive real number. Then*

$$\|\tilde{L}_N^{-1}\|_2 \leq \frac{1}{\varepsilon}O(1), \qquad 0 < p < 1,$$

and

$$\|\tilde{L}_N^{-1}\|_2 \leq O(h^{3p-4}), \qquad p \geq 1.$$

Proof. Let $\tilde{\alpha} = -r_j^-/r_j^c$ and $\tilde{\beta} = -r_j^+/r_j^c$. Then from (4.3) and using Lemma 3, this choice of $\tilde{\alpha}$ and $\tilde{\beta}$ satisfies the assumptions of Lemma 5 ($\tilde{\alpha}+\tilde{\beta} = 1, \tilde{\alpha}, \tilde{\beta} \geq 0$).
Hence, the difference matrix $\tilde{L}_N$ in $(4.1 - 4.3)$ can be written as following

$$\tilde{L}_N = \frac{\varepsilon}{h^2}r_j^c\Big(-\tilde{\alpha}E + I - \tilde{\beta}E^T\Big)$$

where E and I are the matrices defined in Lemma 5. Therefore, from Lemma 5, we obtain

$$\|\tilde{L}_N^{-1}\|_2 = \frac{h^2}{\varepsilon|r_j^c|}\|A^{-1}\|_2 \leq \frac{h^2}{\varepsilon|r_j^c|}\,O\big((N-1)^2\big) = \frac{1}{\varepsilon|r_j^c|}\,O(1),$$

From (4.3), $|r_j^c|$ can be written as

$$|r_j^c| = 24 + \frac{5}{2}\xi^2 + \frac{1}{4}\xi^3 + \frac{1}{8}\xi^4 = \frac{192\varepsilon^4 + 20\tilde{a}^2h^2\varepsilon^2 + 2\tilde{a}^3h^3\varepsilon + \tilde{a}^4h^4}{8\varepsilon^4}$$

Substituting from the equation above, we get

$$\|\tilde{L}_N^{-1}\|_2 \leq \frac{8\varepsilon^3}{192\varepsilon^4 + 20\tilde{a}^2h^2\varepsilon^2 + 2\tilde{a}^3h^3\varepsilon + \tilde{a}^4h^4}\,O(1)$$

Using the fact that $\tilde{a}$ is a constant and the assumption $\varepsilon = O(h^p)$ for a positive number p. we obtain

$$\frac{8\varepsilon^3}{192\varepsilon^4 + 20\tilde{a}^2h^2\varepsilon^2 + 2\tilde{a}^3h^3\varepsilon + \tilde{a}^4h^4} = \frac{O(h^{3p})}{O(h^{4p}) + O(h^{2+2p}) + O(h^{3+p}) + O(h^4)}$$

(i) if $0 < p < 1$, then

$$\|\tilde{L}_N^{-1}\|_2 \leq \frac{O(h^{3p})}{O(h^{4p})} = \frac{1}{\varepsilon}\,O(1)$$

(ii) if $p \geq 1$, then

$$\|\tilde{L}_N^{-1}\|_2 \leq \frac{O(h^{3p})}{O(h^4)} = O(h^{3p-4})$$

□

5. Numerical Examples and Discussion

In this section, we present results corresponding to the numerical solution of the test problems via applying the proposed method defined in Section 3. Both cases of boundary layer, on the left side as well as right side are discussed. The computational results are given in the form of tables and figures. These results are listed with the maximum absolute error and rate of convergence for different values of ε and N.

For given value of N, the maximum absolute errors and the corresponding rate of convergence are calculated as

$$E^N = \max_{0\le j\le N} |u(x_j) - U_j|, \qquad \text{and} \qquad r^N = \log_2\Big(\frac{E^N}{E^{2N}}\Big),$$

where $u(x_j)$ is the exact solution and U_j is the numerical solution. In the case of the exact solution is not known, the maximum absolute error and the corresponding rate of convergence is evaluated using the double mesh principle [3]

$$\tilde{E}^N = \max_{0\le j\le N} |U_j^N - U_j^{2N}|, \qquad \text{and} \qquad \tilde{r}^N = \log_2\Big(\frac{\tilde{E}^N}{\tilde{E}^{2N}}\Big).$$

Example 1.

$$\varepsilon u_\varepsilon''(x) + u_\varepsilon'(x) - 2u_\varepsilon(x-\delta) - 5u_\varepsilon(x) + u_\varepsilon(x+\eta) = 0, \qquad x \in (0,1)$$

with the interval conditions

$$u_\varepsilon(x) = 1, \qquad -\delta \le x \le 0, \qquad u_\varepsilon(x) = 0, \quad 1 \le x \le 1+\eta.$$

The exact solution is given by

$$u_\varepsilon(x) = \frac{\exp(m_1 x + m_2) - \exp(m_1 + m_2 x)}{\exp(m2) - \exp(m_1)}$$

where $m_{1,2} = (-b \pm \sqrt{b^2 - 4ac})/2a$, $a = \varepsilon + (\eta^2 - 2\delta^2)/2$, $b = 1 + 2\delta + \eta$ and $c = -6$.

Example 2.

$$\varepsilon u_\varepsilon''(x) + u_\varepsilon'(x) + 2u_\varepsilon(x-\delta) - 3u_\varepsilon(x) = 0, \qquad x \in (0,1)$$

with the interval and boundary conditions

$$u_\varepsilon(x) = 1, \qquad -\delta \le x \le 0, \qquad u_\varepsilon(1) = 1.$$

The boundary layer is at $x = 0$ and the exact solution is not known.

Example 3.

$$\varepsilon u_\varepsilon''(x) - u_\varepsilon'(x) - 2u_\varepsilon(x-\delta) + 3u_\varepsilon(x) - 2u_\varepsilon(x+\eta) = 0, \qquad x \in (0,1)$$

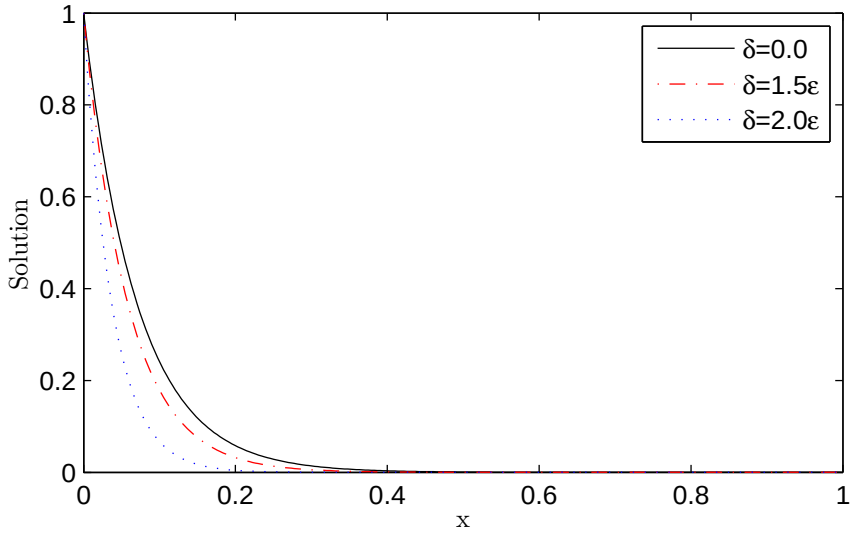

Figure 1: Effect of δ on the solution of Example 1 for $\varepsilon = 10^{-1}$.

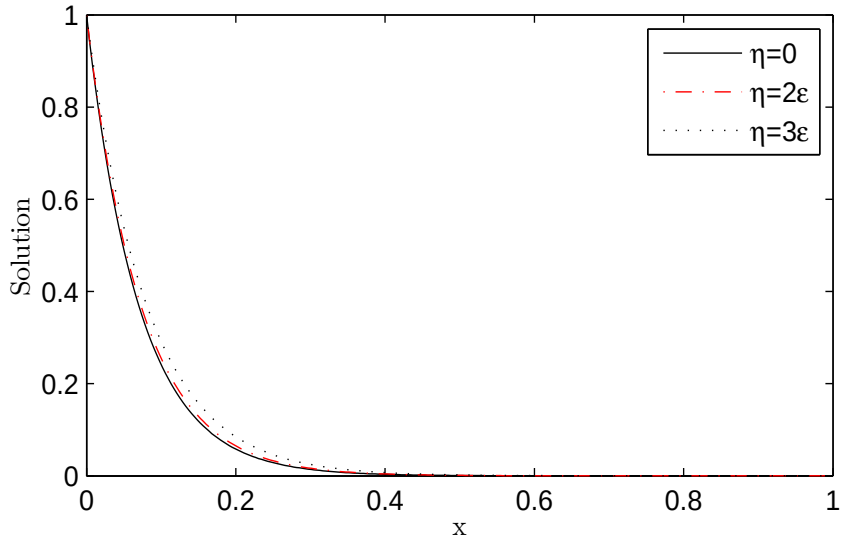

Figure 2: Effect of η on the solution of Example 1 for $\varepsilon = 10^{-1}$.

ε	Number of mesh points N				
	64	128	256	512	1024
1	8.517E−9	5.363E−10	3.387E−11	1.948E−12	4.564E−13
	3.989	3.985	4.120	2.094	
10^{-2}	1.935E−3	2.302E−4	2.638E−5	2.724E−6	1.746E−7
	3.071	3.126	3.276	3.964	
10^{-4}	1.799E−3	2.161E−4	2.438E−5	2.500E−6	2.416E−7
	3.058	3.148	3.285	3.371	
10^{-6}	1.798E−3	2.160E−4	2.436E−5	2.498E−6	2.414E−7
	3.058	3.148	3.286	3.371	
10^{-8}	1.798E−3	2.160E−4	2.436E−5	2.498E−6	2.414E−7
	3.058	3.148	3.286	3.371	
10^{-10}	1.799E−3	2.160E−4	2.436E−5	2.498E−6	2.414E−7
	3.058	3.148	3.286	3.371	

Table 1: The values of E^N and r^N for Example 1

	δ	$N = 64$	$N = 128$	$N = 256$	$N = 512$	$N = 1024$
$\varepsilon = 10^{-1}$	0.5ε	1.972E−06	1.260E−07	7.975E−09	5.014E−10	3.140E−11
	1.5ε	8.950E−06	5.751E−07	3.648E−08	2.299E−09	1.444E−10
	2.0ε	3.145E−05	2.059E−06	1.311E−07	8.285E−09	5.204E−10
$\varepsilon = 10^{-2}$	0.5ε	1.908E−03	2.272E−04	2.601E−05	2.685E−06	1.721E−07
	2.5ε	2.767E−03	3.312E−04	3.806E−05	3.981E−06	2.564E−07
	3.0ε	3.188E−03	3.896E−04	4.466E−05	4.658E−06	2.992E−07
$\varepsilon = 10^{-3}$	0.5ε	1.809E−03	2.171E−04	2.452E−05	2.516E−06	2.432E−07
	2.5ε	1.879E−03	2.252E−04	2.549E−05	2.619E−06	2.531E−07
	3.0ε	1.906E−03	2.284E−04	2.587E−05	2.658E−06	2.570E−07

Table 2: The values of E^N for Example 1 for different values of ε and δ.

with the interval conditions

$$u_\varepsilon(x) = 1, \quad -\delta \le x \le 0, \qquad\qquad u_\varepsilon(x) = -1, \quad 1 \le x \le 1 + \eta.$$

The exact solution of this problem is not known and the boundary layer occurs near the right end of interval.

ε	Number of mesh points N				
	64	128	256	512	1024
10^{-1}	3.777E−7	2.402E−8	1.511E−9	8.602E−11	5.944E−11
	3.975	3.990	4.135	1.563	
10^{-2}	1.011E−3	1.218E−4	1.376E−5	1.412E−6	9.042E−8
	3.053	3.146	3.284	3.965	
10^{-4}	1.046E−3	1.235E−4	1.346E−5	1.240E−6	1.060E−7
	3.081	3.198	3.440	3.548	
10^{-6}	1.046E−3	1.237E−4	1.350E−5	1.260E−6	9.137E−8
	3.081	3.195	3.421	3.786	
10^{-8}	1.046E−3	1.237E−4	1.350E−5	1.260E−6	9.249E−8
	3.081	3.195	3.421	3.768	
10^{-10}	1.046E−3	1.237E−4	1.352E−5	1.274E−6	1.043E−7
	3.081	3.194	3.409	3.610	

Table 3: The values of $\tilde{E}^N$ and $\tilde{r}^N$ for Example 2.

ε	$N = 64$	$N = 128$	$N = 256$	$N = 512$	$N = 1024$
2^{-2}	1.337E−08	8.418E−10	5.508E−11	7.102E−12	8.878E−13
2^{-4}	3.620E−06	2.315E−07	1.465E−08	9.273E−10	5.217E−11
2^{-6}	8.285E−04	5.539E−05	3.597E−06	2.296E−07	1.451E−08
2^{-8}	8.847E−04	1.064E−04	1.203E−05	1.238E−06	1.201E−07
2^{-10}	6.637E−04	7.821E−05	7.958E−06	7.446E−07	7.529E−08
2^{-12}	2.371E−04	2.764E−05	2.438E−06	5.038E−07	1.313E−07
2^{-14}	1.517E−04	6.058E−06	1.576E−06	4.276E−07	1.256E−07

Table 4: The values of $\tilde{E}^N$ for Example 2 for $\delta = 0.01$ and different values of ε

Table 1 displays the values of E^N and r^N for $\delta = \eta = 0.5\varepsilon$ and for different values of ε, whereas, Table 2 contains the maximum absolute errors E^N for different values of ε and δ. It is clear that the proposed method is ε-uniformly convergent, and the maximum absolute errors E^N decrease rapidly with increasing N.

Figs 1 and 2 represent the numerical solution of Example 1 for different values of delay and advance parameters, respectively. These Figures indicate that as δ increases the thickness of the boundary layer decreases and decreases when η increases.

Table 3 shows the values of $\tilde{E}^N$ and $\tilde{r}^N$ for Example 2 with $\delta = 0.5\varepsilon$ for different values of ε. The numerical results represented in this Table clearly

show that the proposed method is ε-uniformly convergent and has accuracy of order three. Table 4 contains the values of $\tilde{E}^N$ for Example 2 due to the present method. It is clear that the present method approximates the exact solution very well and the maximum absolute errors decrease rapidly as N increases.

In Table 5, the values of $\tilde{E}^N$ and $\tilde{r}^N$ for Example 3 are computed for $\delta = \eta = 0.5\varepsilon$ and different values of ε. Table 6 clearly shows the uniform convergence in different values of η and ε. Figs 3 and 4 show the impact of small shifts on the solution. It is observed that the thickness of the layer increases as the delay parameter δ increases while it decreases when the advance parameter η increases.

Comparisons of our results with the numerical results given in [8, 9] and [15] have been made and tabulated in Tables 7 and 8, respectively. The superiority of the present method over the previous ones is clear.

	Number of mesh points N				
ε	64	128	256	512	1024
10^{-1}	2.304E−6	1.460E−7	9.179E−9	5.768E−10	4.146E−11
	3.981	3.991	3.992	3.798	
10^{-2}	3.434E−3	3.969E−4	4.411E−5	4.490E−6	2.860E−7
	3.113	3.170	3.296	3.973	
10^{-4}	3.375E−3	3.936E−4	4.415E−5	4.649E−6	5.039E−7
	3.100	3.156	3.248	3.206	
10^{-6}	3.374E−3	3.934E−4	4.407E−5	4.607E−6	4.794E−7
	3.100	3.158	3.258	3.265	
10^{-8}	3.374E−3	3.934E−4	4.407E−5	4.607E−6	4.622E−7
	3.100	3.158	3.258	3.317	
10^{-10}	3.374E−3	3.934E−4	4.395E−5	3.954E−6	1.543E−6
	3.100	3.162	3.475	1.358	

Table 5: The values of $\tilde{E}^N$ and $\tilde{r}^N$ for Example 3.

	η	$N = 64$	$N = 128$	$N = 256$	$N = 512$	$N = 1024$
$\varepsilon = 10^{-1}$	0.5ε	3.096E−06	1.959E−07	6.174E−08	3.876E−09	6.924E−10
	1.5ε	6.763E−06	4.338E−07	7.202E−08	4.351E−09	9.503E−10
	2.0ε	5.751E−05	3.683E−06	2.331E−07	1.466E−08	9.339E−10
$\varepsilon = 10^{-2}$	0.5ε	3.544E−03	4.092E−04	5.343E−05	5.459E−06	2.150E−07
	2.5ε	5.279E−03	5.980E−04	6.782E−05	6.963E−06	4.461E−07
	3.0ε	6.136E−03	7.024E−04	7.894E−05	8.167E−06	5.227E−07
$\varepsilon = 10^{-3}$	0.5ε	3.394E−03	3.970E−04	4.592E−05	4.824E−06	1.850E−07
	2.5ε	3.533E−03	4.123E−04	4.699E−05	4.938E−06	4.694E−07
	3.0ε	3.586E−03	4.182E−04	4.767E−05	5.010E−06	4.764E−07

Table 6: The values of $\tilde{E}^N$ for Example 3 for different values of ε and η.

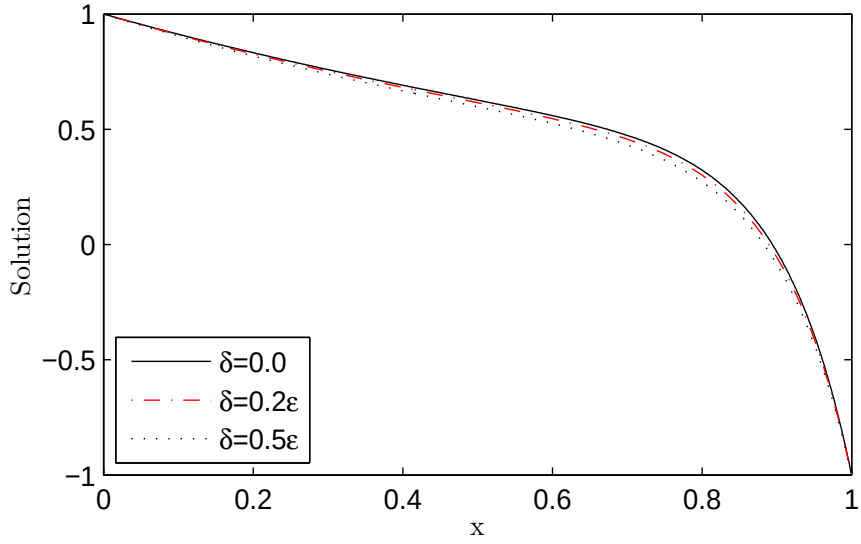

Figure 3: Effect of δ on the solution of Example 3 for $\varepsilon = 10^{-1}$.

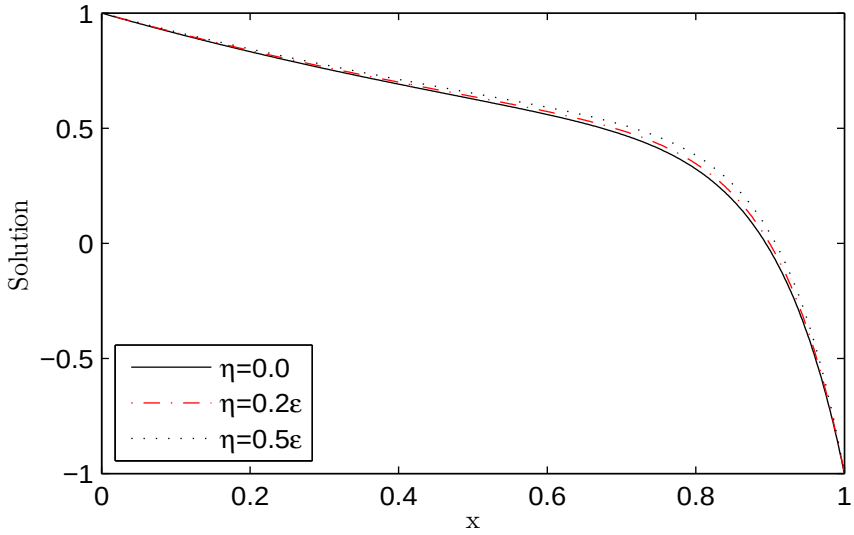

Figure 4: Effect of η on the solution of Example 3 for $\varepsilon = 10^{-1}$.

N →	64		256		1024	
$\varepsilon \downarrow$	Method [15]	Our method	Method [15]	Our method	Method [15]	Our method
1	5.240E−3	4.616E−7	1.345E−3	1.839E−9	3.385E−4	7.221E−12
10^{-2}	3.480E−2	1.823E−3	9.996E−3	2.483E−5	2.583E−3	1.641E−7
10^{-8}	5.717E−2	1.798E−3	1.898E−2	2.436E−5	5.944E−3	2.414E−7
10^{-10}	5.717E−2	1.799E−3	1.898E−2	2.436E−5	5.944E−3	2.414E−7

Table 7: E^N for Example 1 using the proposed method and the method in [15].

	$\varepsilon = 2^{-3}$		$\varepsilon = 2^{-10}$		$\varepsilon = 2^{-20}$	
$N \rightarrow$	256	1024	256	1024	256	1024
Method [8]	3.240E−3	8.172E−4	1.498E−2	4.784E−3	1.484E−2	4.579E−3
Method [9]	1.806E−5	1.129E−6	1.443E−4	1.413E−5	1.461E−4	1.418E−5
Our Method	7.124E−10	3.780E−12	1.316E−5	1.241E−7	1.350E−5	9.138E−8

Table 8: Comparison of maximum absolute error for Example 2 with $\delta = 0.3\,\varepsilon$.

6. Conclusions

An efficient numerical method based on non-uniform mesh has been developed for solving numerically the singularly perturbed differential difference equations with small delay and advance parameters. Both cases, when the boundary layer occurs in the left and in the right side of interval are studied. The truncation error and the stability of this method are discussed. The advantages of the proposed method are the higher order of accuracy and it is simple to implement.

The impact of small shifts on the layer behavior of the solution has been discussed by considering both cases of boundary layers. It is observed that in the case of left boundary layer, the thickness of the layer decreases as the delay parameter δ increases while it increases when the advance parameter η increases. In the right boundary layer, the impact of these shifts is reverse, i.e., as δ increases, the thickness of the boundary layer increases and decreases when η increases. The produced results are also seen to be more accurate if compared with some available results given in the literature.

Acknowledgments

The authors are indebted to Professor S.E. El-Gendi and Professor H.M. El-Hawary for their valuable suggestions and constructive criticism.

References

[1] A. Bellen, M. Zennaro, *Numerical Methods for Delay Differential Equations*, Oxford University Press, Oxford (2003).

[2] A.E. Berger, J.M. Solomon, M. Ciment, S.H. Leventhal, B.C. Weinberg, Generalized OCI schemes for boundary layer problems, *Math. Comput.*, **35** (1980), 695-731.

[3] E.R. Doolan, J.J.H. Miller, W.H.A. Schilders, *Uniform Numerical Methods for Problems with Initial and Boundary Layers*, Boole Press, Dublin (1980).

[4] V.Y. Glizer, Asymptotic analysis and solution of a finite-horizon H_∞ control problem for singularly-perturbed linear systems with small state delay, *J. Optim. Theory Appl.*, **117** (2003), 295-325.

[5] E. Isaacson, H.B. Keller, *Analysis of Numerical Methods*, Wiley, New York (1994).

[6] M. K. Kadalbajoo, K. C. Patidar, K. K. Sharma, ϵ-Uniformly convergent fitted methods for the numerical solution of the problems arising from singularly perturbed general DDEs, *Appl. Math. Comput.*, **182** (2006), 119-139.

[7] M.K. Kadalbajoo, K.K. Sharma, Numerical analysis of boundary-value problems for singularly perturbed differential-difference equations with small shifts of mixed type, *J. Optim. Theory Appl.*, **115**, No. 1 (2002), 145-163.

[8] M.K. Kadalbajoo, K.K. Sharma, An ϵ-uniform convergent method for a general boundary-value problem for singularly perturbed differential-difference equations: Small shifts of mixed type with layer behavior, *J. Comput. Methods Sci. Eng.*, **6** (2006), 39-55.

[9] M. K. Kadalbajoo, A.S. Yadaw, An ϵ-Uniform Ritz-Galerkin finite element method for numerical solution of singularly perturbed delay differential equations, *Int. J. Pure Appl. Math.*, **55** (2009), 265-286.

[10] Y. Kuang, *Delay Differential Equations with Applications in Population Dynamics*, Academic Press, Boston (1993).

[11] C.G. Lange, R.M. Miura, Singular perturbation analysis of boundary-value problems for differential difference equations, V. Small shifts with layer behavior, *SIAM J. Appl. Math.*, **54** (1994), 249-272.

[12] C.G. Lange, R.M. Miura, Singular perturbation analysis of boundary-value problems for differential difference equations, VI. Small shifts with rapid oscillations, *SIAM J. Appl. Math.*, **54** (1994), 273-283.

[13] A. Longtin, J. Milton, Complex oscillations in the human pupil light reflex with mixed and delayed feedback, *Math. Biosci.*, **90** (1988), 183-199.

[14] J.J.H. Miller, E. O'Riordan, G.I. Shishkin, *Fitted Numerical Methods For Singular Perturbation Problems*, World Scientific, Singapore (1996).

[15] J. Mohapatra, S. Natesan, Uniformly convergent numerical method for singularly perturbed differential-difference equation using grid equidistribution, *Int. J. Numer. Meth. Biomed. Engng.*, **27** (2011), 1427-1445.

[16] R.E. O'Malley, *Singular Perturbation Methods for Ordinary Differential Equations*, Springer-Verlag, New York (1991).

[17] Y. Qiu, D.M. Sloan, T. Tang, Numerical solution of a singularly perturbed two-point boundary-value problem using equidistribution: Analysis of convergence, *J. Comput. Appl. Math.*, **116** (2000), 121-143.

[18] H.G. Roos, M. Stynes, L. Tobiska, *Numerical Methods for Singularly Perturbed Differential Equations*, Springer-Verlag, Berlin (1996).

[19] A.A. Salama, *The Operator Compact Implicit Methods for the Numerical Treatment of Ordinary Differential and Integro-differential Equation*, Ph.D. Thesis, Assiut University, Assiut (1992).

[20] A. Segal, Aspects of numerical methods for elliptic singular perturbation problems, *SIAM J. Sci. Stat. Comput.*, **3** (1982), 327-349.

[21] M. Wazewska-Czyzewska, A. Lasota, Mathematical models of the red cell system, *Mat. Stosow*, **6** (1976), 25-40.